Enhanced efficacy of porcine lung surfactant extract by utilization of its aqueous swelling dynamics.

Larsson, Marcus; Haitsma, Jack J; Lachmann, Burkhard; Larsson, Kåre; Nylander, Tommy; Wollmer, Per

Published in:
Clinical Physiology and Functional Imaging

DOI:
10.1046/j.1475-097X.2002.00397.x

2002

Clin Physiol & Func Im (2002) **22,** pp39–48

Enhanced efficacy of porcine lung surfactant extract by utilization of its aqueous swelling dynamics

Marcus Larsson[1,2], Jack J. Haitsma[2], Burkhard Lachmann[2], Kåre Larsson[3], Tommy Nylander[4] and Per Wollmer[1]

[1]*Department of Clinical Physiology, Lund University, Malmö, Sweden,* [2]*Department of Anesthesiology, Erasmus University, Rotterdam, the Netherlands,* [3]*Camurus Lipid Research Foundation, Ideon Science Park, Lund, Sweden, and* [4]*Physical Chemistry 1, Lund University, Lund, Sweden*

Correspondence

Marcus Larsson, Department of Clinical Physiology, Lund University, S-205 02 Malmö, Sweden
Fax: +46 40336620
e-mail: M.Larsson@klchem.se

Accepted for publication

Received 22 August 2001;
accepted 30 October 2001

Keywords:

porcine lung surfactant; surfactant administration; surfactant swelling dynamics

Summary

This study investigates the interactions between a porcine lung surfactant (PLS) extract and distilled water, saline solution or Ringer solution. The phases which coexist in equilibrium with water or electrolyte solutions were analysed by X-ray diffraction and cryo transmission electron microscopy (cryo-TEM). A lamellar phase with a structure unit consisting of double bilayers was observed in water, whereas lamellar phases with the usual bilayer structure unit were formed in saline and in Ringer solutions. At 25°C the presence of a 4·2-Å peak in the X-ray diffraction wide-angle region of these three maximally swollen phases showed that most of the hydrocarbon chains were organized in a crystalline packing. At 42°C the chains in all three phases were melted which, in combination with the low-angle diffraction, shows that they were liquid-crystalline. Polyhedral-like vesicles and spherically shaped multilamellar vesicles were observed in cryo-TEM. The bilayer unit structures were consistent with the periodicity seen by X-ray diffraction. The dynamic swelling behaviour was followed in the polarizing microscope. A remarkable growth of birefringent networks was seen at the air interface of samples swollen in Ringer solution and saline solution. No such interfacial growth phenomena were observed during swelling in water without electrolytes. Then, these dynamics were analysed in relation to time-dependent pulmonary administration of the surfactant extract in rats. Variation in the time of administration (20 and 60 min) after mixing the extract with saline or Ringer solution showed clear differences in physiological effects. At pulmonary administration when the swelling behaviour *in vitro* showed a maximum in dynamics, the arterial oxygenation was superior to that of administration at a time after a steady-state had been reached. This means that the clinical performance of mammalian lung surfactant extracts can be significantly improved by taking the time-dependent aqueous swelling of the extract into account.

Introduction

Pulmonary surfactant covers the alveoli as an aqueous film, reducing surface tension which prevents collapse of alveoli at the end of the expiration and thus allows effortless breathing (Gommers & Lachmann, 1993). In premature infants with surfactant deficiency (respiratory distress syndrome), treatment with exogenous surfactant has shown to be a life-saving therapy.

In surfactant replacement therapy, synthetic lipid formulations or extracts prepared from mammalian alveolar surface layers are used (Boncuk-Dayanikli & Teusch, 1995). An example of a commercially available synthetic lipid-detergent mixture is Exosurf, which consists of dipalmitoylphosphatidylcholine (DPPC) (85%), hexadecylalcohol (9%) and the detergent Tyloxapol (6%). In the preparation of surfactants from mammalian lungs, extraction by organic solvents is used. Then, besides phospholipids, the preparation will also contain the hydrophobic surfactant proteins SP-B and SP-C.

There are numerous reports on surface tension and dynamics of surface film formation of surfactant formulations relevant to surfactant replacement therapy. Only limited information is available, however, on the ultrastructure of the phospholipids in the hypophase (Reiss *et al.*, 1984; Amrein *et al.*, 1997; von Nahmen *et al.*, 1997). Therefore, this study explores the interactions between a porcine lung surfactant extract (PLS)

and aqueous solution and physiological electrolyte solutions. The primary aim of this investigation was to identify the phases formed in equilibrium with distilled water, with saline solution, and with Ringer solution, by means of X-ray diffraction and cryo transmission electron microscopy (cryo-TEM), and to study the swelling behaviour of the PLS in electrolyte solutions and in pure water by means of polarizing microscopy. As a most remarkable dynamic swelling behaviour was found in electrolyte solutions but not in water, a secondary aim was to investigate whether or not these features of the swelling dynamics had significance at pulmonary administration.

Methods

Surfactant preparation

All experiments were performed with a PLS extract (Leo Pharmaceutical Products, Ballerup, Denmark) prepared from freshly slaughtered pigs (Gommers *et al.*, 1993). PLS was extracted from minced porcine lungs, according to the classical extraction method of Bligh & Dyer (1959). The chloroform phase was evaporated and neutral lipids were removed by acetone. The preparation was finally freeze-dried. Besides hydrophobic proteins and phospholipids, the extract contained a few percent cholesterol, free fatty acids and fatty acid glycerides.

Aqueous formulation of the extract

Aqueous samples of PLS were prepared by adding varying proportions of water, physiological saline solution or Ringer solution in glass test tubes, which were gently shaken to facilitate mixing and interaction towards equilibrium. Ringer-acetate (Na^+ 130 mmol, K^+ 4 mmol, Ca^{2+} 2 mmol, Mg^{2+} 1 mmol, Ac^- 30 mmol, Cl^- 100 mmol) (Pharmacia & Upjohn, Uppsala, Sweden) was used.

In vitro structural studies

Aliquots of freshly prepared or equilibrated samples were transferred to microscope slides for examination either during swelling of the dry PLS powder or after equilibrium had been reached. Observations in the microscope were performed at 25°C and at 42°C. Other aliquots of equilibrated samples were used for cryo-TEM and for X-ray diffraction experiments at 25°C and 42°C.

A Leitz polarizing microscope was used with a Sony CCD camera (UP2300P and PUM-14N1E Sony Corp., Tokyo, Japan) and colour printer. X-ray data were obtained by using a Kratky compact system equipped with a two-position sensitive detector, with 1024 channels of width 53·6 m (OED 50 M from Mbraun, Graz, Austria). The small-angle detector was placed at distance of 27·7 cm from the sample, while wide-angle detector was placed at an angle of 20·2° with a sample- to-detector distance of 29·7 cm. The CuK_α nickel-filtered radiation of wavelength 1·542° was provided by a Seifert IF 300 X-ray generator (Seifert X-ray Co., PA, USA) operating at 50 kV and 40 mA. Temperature control of the sample within 0·1°C was achieved by using a Peltier element.

Samples were deposited on cryo-TEM grids and immediately thereafter plunged into liquid ethane (−180°C). The sample was viewed in a Philips Bio-twin 120 cryo (Philips, Eindhover, The Netherlands) with an La_2B_6 filament. The cryo sample was at all times kept below −160°C.

Animal protocol

The protocol was approved by the local Animal Committee of the Erasmus University Rotterdam; care and handling of the animals were in accord with the NIH guidelines.

Sixteen male Sprague–Dawley rats (Harlan CPB, Zeist, the Netherlands) bodyweight (BW) 240–320 g, were anaesthetized with nitrous oxide, oxygen and isoflurane (65/33/2%), tracheotomized and a catheter was inserted into a carotid artery. Anaesthesia was maintained with pentobarbital sodium (Nembutal; Algin BV, Maassluis, the Netherlands) 60 mg kg^{-1} h^{-1} i.p. injections; neuromuscular block was produced with pancuronium bromide (Pavulon; Organon Technika, Boxtel, the Netherlands) 2·0 mg kg^{-1} h^{-1} i.m. Body temperature was kept within normal range by means of a heating pad.

Rats were connected to a ventilator (Servo Ventilator 300, Siemens-Elema, Solna, Sweden) and ventilated with pure oxygen in a pressure-controlled mode, frequency 30 bpm, an I/E ratio of 1:2, a peak airway pressure (PIP) of 12 cm H_2O and a positive end-expiratory pressure (PEEP) of 2 cm H_2O. Initially, PIP was increased to 20 cm H_2O for 1 min to recruit atelectatic areas. Next, surfactant deficiency was induced by repeated whole-lung lavage (BAL) to achieve a PaO_2 < 85 mmHg (Lachmann *et al.*, 1980). Just before the first lavage, PIP and PEEP were elevated to 26 and 6 cm H_2O, respectively.

Treatment consisted of: exogenous surfactant (35 mg kg^{-1} bodyweight dissolved in saline 25 mg ml^{-1}). The PLS saline mixture was repeatedly drawn in and out of a syringe during 0·5 min. One group of eight rats received surfactant 20 min after preparation of the surfactant mixture and the other group of eight rats received surfactant 60 min after preparation of the surfactant mixture. Surfactant suspension (4 ml kg^{-1} BW ± 0·4 ml) was administered directly into the endotracheal tube followed by a bolus of air (14 ml kg^{-1}) (ventilator settings were not changed).

Blood samples for measurement of PaO_2 and $PaCO_2$ were taken from the carotid artery before BAL and 5 min after the last lavage (directly followed by treatment) and at the following times 5, 15, 30, 60, 90 and 120 min after surfactant administration (ABL$^{TM.}$ 505, Radiometer A/S, Copenhagen, Denmark).

After the experiments, the animals were killed with an overdose of pentobarbital sodium.

Statistical analysis

Statistical analysis was performed utilizing the SPSS 10·0 statistical software package (SPSS Inc., Chicago, IL, USA). Inter-group comparisons were analysed with ANOVA. Intra-group comparisons were analysed with repeated measures ANOVA. If ANOVA resulted in $P<0·05$ a Tukey posthoc test was performed. Statistical significance was accepted at $P<0·05$.

Results

Phase behaviour of the surfactant extract in water and in physiological electrolyte solutions

The physiological situation corresponds to an aqueous content of lung surfactants of about 90%. We have also studied samples with much lower water content, as we need to reach the one-phase region in the water composition diagram to obtain X-ray diffraction data, which can unambiguously identify the structure. A first overview of samples with varying compositions indicated that a one-phase region exists at about 50% of water, and at dilution of this phase colloidal dispersions are formed.

Polarizing microscopy

A sample of 50% (w/w) PLS powder in water, which was equilibrated at room temperature for 20 h is shown in Fig. 1. A 'woven' pattern is observed. Such birefringent textures are often seen in the gel phases of lipid–water samples, and the bilayer of gel phases contains crystalline hydrocarbon chains (Larsson & Quinn, 1994). This composition is close to the limit of swelling of this phase (see X-ray data below). Above the limit of swelling, aggregates with a texture characteristic for liposomes start to form. A sample containing 90% of water, exhibiting the so-called Maltesi-cross typical for spherically concentric lipid bilayers, is shown in Fig. 2.

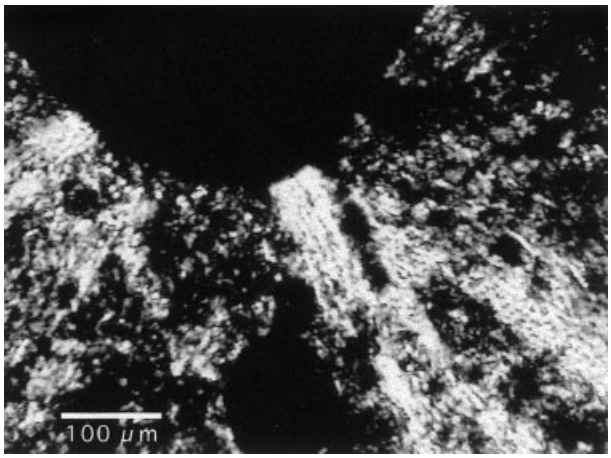

Figure 1 A sample of PLS with 50% (w/w) of water viewed in the polarizing microscope.

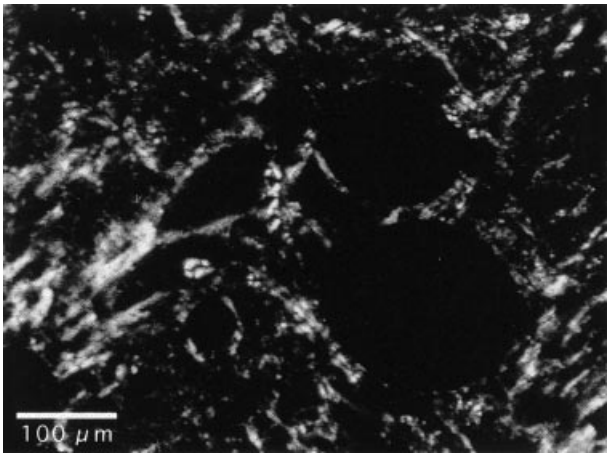

Figure 2 A sample of PLS with 90% (w/w) of Ringer solution viewed in its centre region in the polarizing microscope in the beginning of the swelling process. Black circular regions are air bubbles. A lamellar body can be seen as the strongly birefringent elliptically shaped particle to the left.

The swelling behaviour of a sample containing 10% (w/w) PLS and 90% Ringer solution, as seen in the polarizing microscope, is shown in Fig. 3. After about 5 min a homogeneous appearance was obtained, the sample was turbid, and particles with a weak birefringence surrounded by the Ringer solution accumulated at the outer boundary of the liquid phase (Fig. 3a). This accumulation is probably an effect of streaming of the liquid induced by putting the cover slip on a droplet of the mixture on the slide. The birefringence increased, followed by a remarkable increase of contact surface area of the liquid phase towards air. Tubular formations were seen at the front of the liquid. The 'growing' tubules formed branches, which successively became birefringent, as shown in Fig. 3(a,b) recorded 5–15 min after sample mixing. The protrusion from the liquid surface towards air (Fig. 3a) can be seen in Fig. 3(b) to form a tree-like structure. Figure 4 shows an overview of the sample front during 'growth' and Fig. 5 shows a surface view after about 30 min in both ordinary light and polarized light. The surface zone had developed into a birefringent complex network. This branching behaviour ended after approximately 40 min, with some variation from one batch to the other.

When PLS was swollen in physiological saline solution there was a similar growth of networks at the interface, although somewhat less pronounced than in Ringer solution. This dynamic behaviour with pronounced surface enlargement towards birefringent network formation was only observed when PLS was swollen in saline or Ringer solution, not with water. Also, when the water was made isotonic by the addition of glycerol, PLS swollen in this solution still lacked the dynamic swelling behaviour shown by the electrolyte solutions.

X-ray diffraction

The limit of swelling of the lamellar phase is slightly above 50% (w/w) in water, and it is somewhat higher in saline solution and Ringer solution.

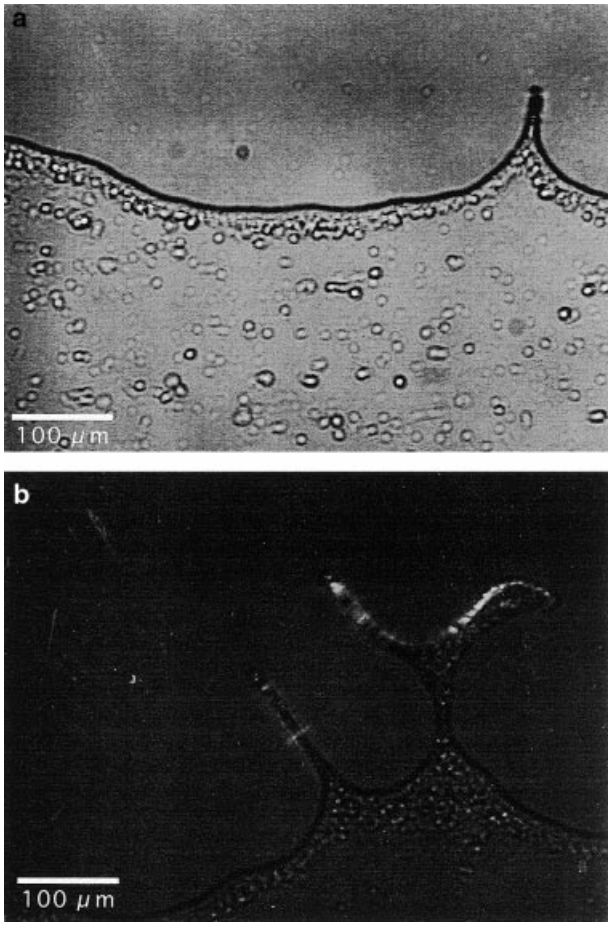

Figure 3 A sample of PLS with 90% (w/w) of Ringer solution viewed in the polarizing microscope. Changes from a to b reflects changes with time from 5 to 15 min after mixing, as viewed at the border towards air. The background is black when polarizer and analyser are crossed (as in b). In order to show the liquid front in the sample more clearly, some deviation of the polarizer plane from 90° in relation to the analyser plane has been applied in a (as seen by the lighter background).

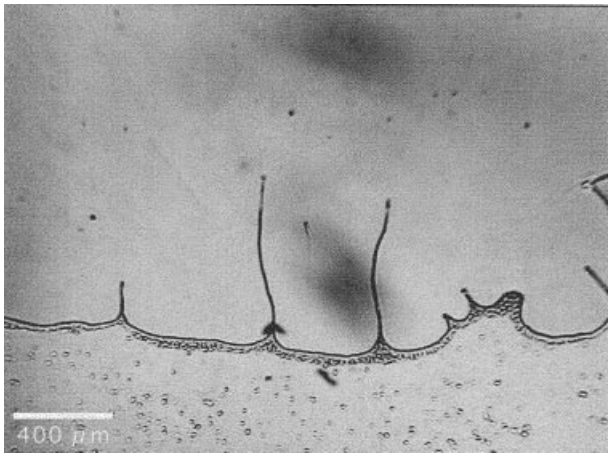

Figure 4 An overview of the surface zone during swelling of a sample of PLS with 90% (w/w) of Ringer solution as seen in ordinary light.

The maximally swollen phase of PLS in distilled water showed diffraction peaks at 25°C at the following spacings, as can be seen in Fig. 6: 117·2° (medium intensity) 59·0° (strong), 39·3° (medium), and about 30° (a weak shoulder). These values correspond to a periodicity of 118° of a lamellar phase. There was a 4·2°- peak in the wide-angle region (not shown in Fig. 6) at 25°C, showing the presence of crystalline chains. Scanning of the wide-angle region at 34, 36 and 38°C showed that the chains become melted at 36°C. At 42°C the lamellar unit period was 104 Å.

The X-ray diffraction pattern of PLS fully swollen in Ringer solution is also shown in Fig. 6. This lamellar phase, containing about 58% water at 25°C has a spacing of 98·5°, and the chains are crystalline. When it is heated to 42°C the chains become liquid and the repetition unit thickness decreases to 86 Å.

A PLS-sample fully swollen in saline solution contains about 55% water; the diffraction curves are shown in Fig. 6. The diffraction pattern recorded at 25°C and 42°C showed the characteristics of a lamellar phase, with a lamellar unit of 90·5 and 83·9°, respectively. The peak corresponding to crystalline chains was seen at 25°C but not at 42°C.

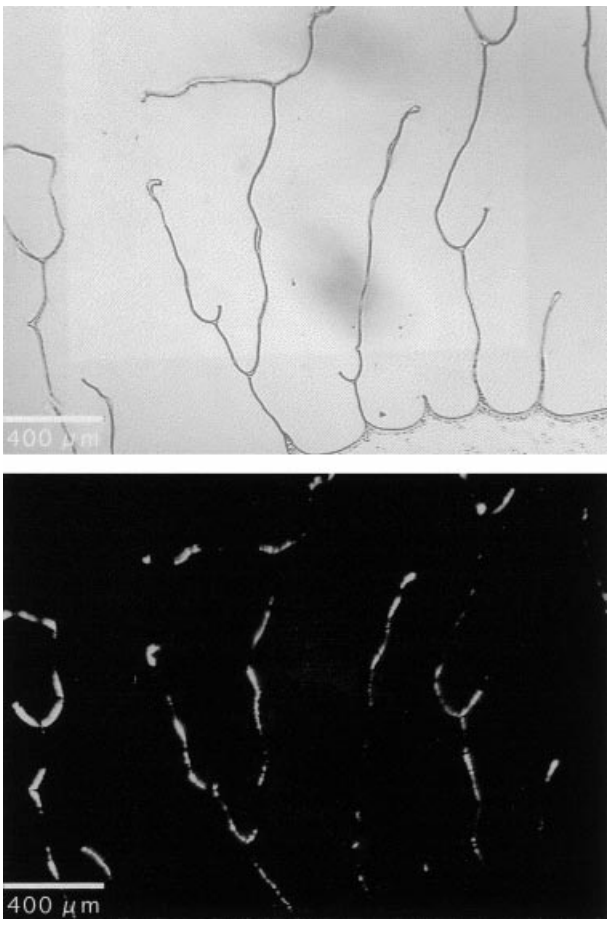

Figure 5 A view of the interface between a PLS sample in 90% Ringer solution and air after half an hour, as seen in ordinary light and the same part in polarized light.

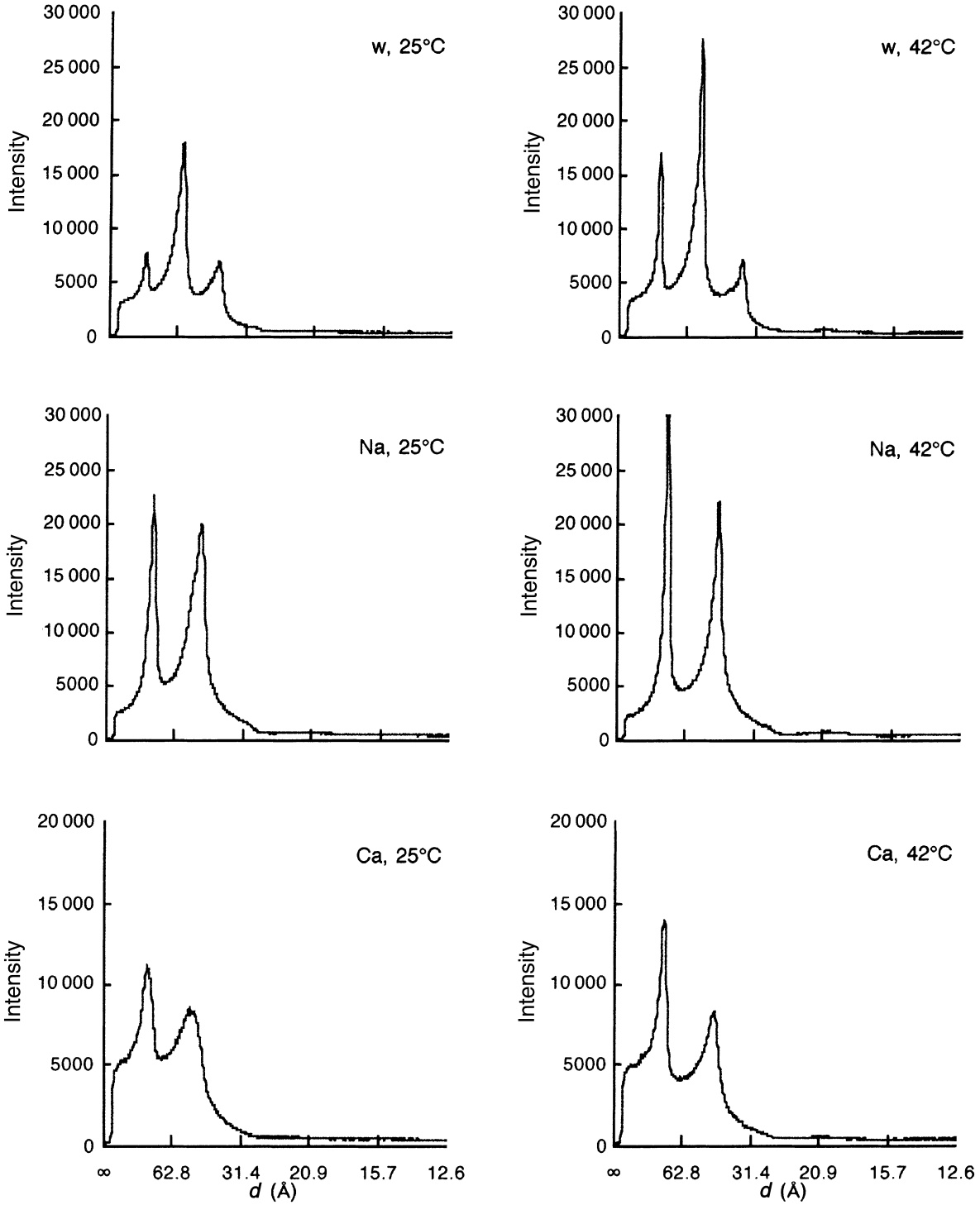

Figure 6 X-ray diraction curves (small-angle region) of dierent aqueous PLS-samples. From above are shown: PLS swollen to its maximum in water at 25°C and at 42°C (denoted w); PLS maximally swollen in Ringer solution at 25°C and at 42°C (denoted Ca); PLS maximally swollen in saline solution at 25°C and at 42°C (denoted Na).

Cryo-TEM

Samples for cryo-TEM were prepared from PLS samples containing both 80% and 90% Ringer solution. Characteristic textures are shown in Fig. 8; multilamellar liposomes and vesicles dominate. In Fig. 7 vesicles consisting of two bilayers can be seen, and adjacent vesicles fuse into a linear structure with a characteristic triple-lamellar unit.

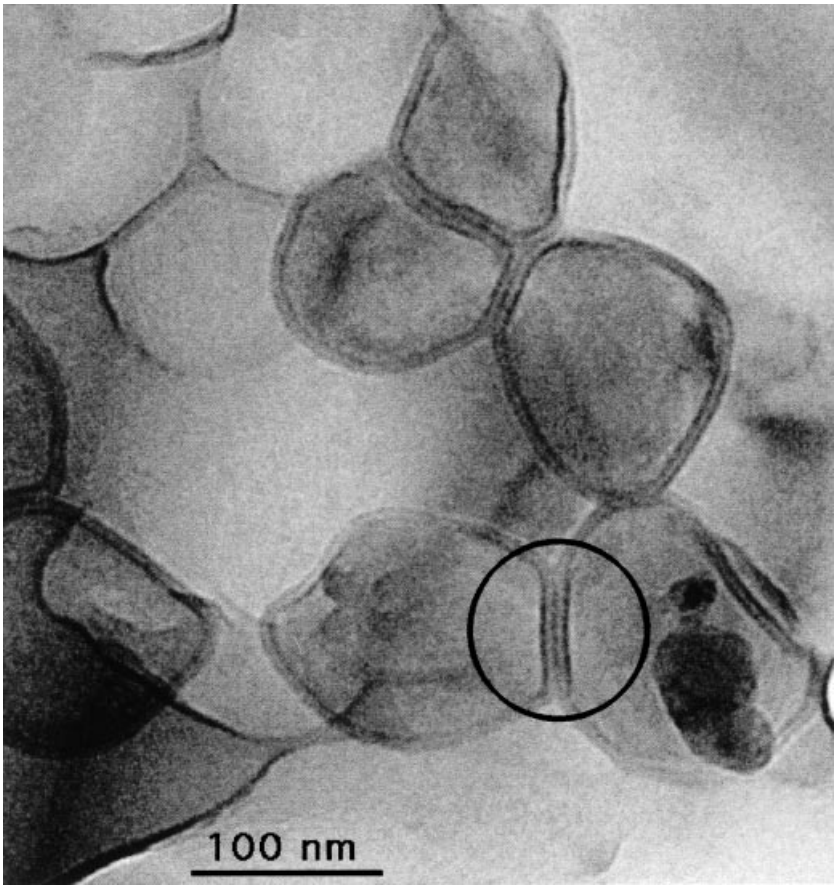

Figure 7 Ultrastructure in cryo-TEM of a PLS-Ringer solution sample with weight ratio 90:10. A circle is drawn around a linear fusion region between two vesicles. The structure represents a transient state of bilayer conformation as vitrification was performed at 5 min after mixing (see discussion).

The liposome-like particles shown in Fig. 8 are similar to the texture of lamellar bodies from the alveoli, which often have been seen in earlier electron microscopy studies.

In vivo evaluation of the significance of the surfactant swelling dynamics

The PLS samples were studied in the polarizing microscope and showed the swelling kinetics described above with formation of birefringent networks. After about 40 min the texture of the PLS saline solution samples had reached a steady-state of swelling; a texture which showed no flow or other textural changes. At about half-time of this process there is a maximum in the dynamics involved in network formation. We therefore used two time windows (20 and 60 min after mixing with saline) to observe whether the *in vitro* interfacial dynamics correlated with *in vivo* surfactant function.

Figure 9 shows the PaO_2 levels over time in both groups which received PLS, dissolved either 20 min or 60 min before administration. After PLS administration PaO_2 improved in both groups, but never reached prelavage levels during the 120 min study period. There was no difference in the PaO_2 levels at 5 min after administration and at the end of the experiment (120 min) in the group which received PLS dissolved 20 min before administration. However, PaO_2 dropped significantly from 5 to 120 min after PLS instillation ($P<0{\cdot}001$) in the group in which PLS was mixed 60 min before administration. Furthermore, the difference in PaO_2 between the two groups at 120 min was also significant ($P<0{\cdot}01$).

A few additional rat experiments were carried out using Ringer solution instead of saline solution, and they showed the same improvement in oxygenation at administration during the maximum in swelling dynamics compared with administration when the swelling dynamics had stopped.

Discussion

According to the swelling behaviour of PLS together with X-ray diffraction and cryo-TEM data, it can be concluded that a lamellar liquid-crystalline phase exists at 50% (w/w) water at 42°C. When the temperature has been lowered to 25°C, chain crystallization has occurred within this phase, as shown by the presence of a 4·2Å peak characterizing the hexagonal chain packing. Above the limit of swelling in electrolyte solution (ranging from 55 to 58%), unilamellar or multilamellar vesicles are formed.

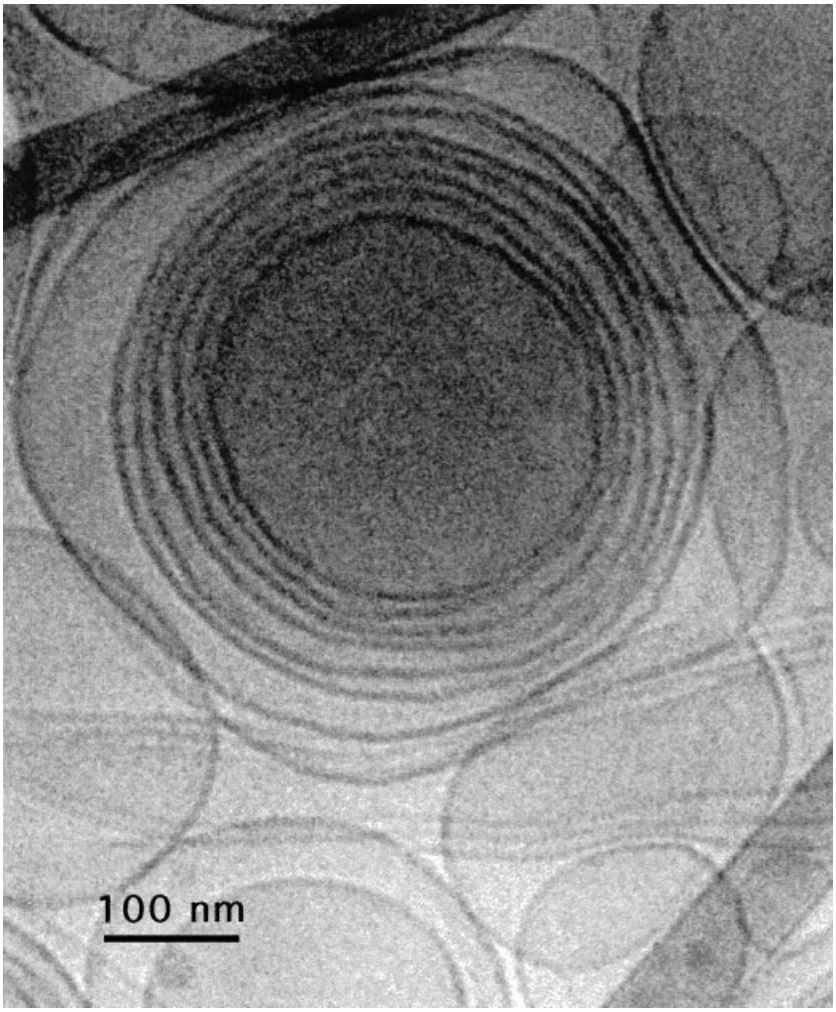

Figure 8 Ultrastructure as seen in cryo-TEM of a PLS-Ringer solution sample with weight ratio 80:20.

There is a major difference, however, between PLS samples swollen in distilled water and those swollen in saline solution or Ringer solution. In water the X-ray diffraction spacings show the characteristic features of lamellar phases, but the unit layer is much thicker in samples swollen in distilled water compared with those swollen in the electrolyte solutions. The lipid bilayer thickness can be estimated from the spacings obtained from the lamellar phases given above. The lamellar liquid-crystalline phase obtained at 42°C of PLS swollen in Ringer solution, for example, gives a bilayer thickness of about 34°, assuming that the density of the bilayer and water layers are the same. This is in good agreement with earlier observations in lipid–water systems. The lamellar periodicity in fully swollen aqueous phases of DPPC above the chain melting temperature, for example, is about 60° (Janiak *et al.*, 1976). This value corresponds to a bilayer thickness of about 35°.

In the present study the lamellar unit thickness observed by X-ray diffraction measurements of PLS in excess of water at 25°C is 118°. This value indicates that the lamellar unit consists of a double bilayer. A lamellar unit period of two lipid bilayers was first reported in a system containing a basic protein from the myelin sheath (Mateu *et al.*, 1973). The authors derived the structure from X-ray data recorded at 20°C. The existence of two bilayers in the repetition unit was proposed to be related to the existence of both crystalline and liquid-like hydrocarbon chains. In their proposed structure there are bilayers with crystalline chains alternating with bilayers with chains in a liquid conformation (Mateu *et al.*, 1973). A similar lamellar structure unit consisting of two bilayers was described later (Gulik *et al.*, 1994) in a study using an extract of bovine lung surfactant lipids. The latter extract must have been different from our PLS preparation, as shown by large differences in X-ray data at maximal swelling. The double-bilayer phase transformed into an ordinary bilayer phase at increased temperature involving chain melting, like that of the nerve myelin system (Mateu *et al.*, 1973), but contrary to our PLS system. Gulik *et al.*'s (1994) proposed structure was different, however, to that of Mateu *et al.* (1973) with monolayers with crystalline chains alternating with monolayers with disordered chains in each bilayer.

The model we derived for the PLS water double bilayer structure at physiological conditions, when all chains have the liquid type of conformation, is shown in Fig. 10. It is

different from the double-bilayer structures proposed earlier (Mateu *et al.*, 1973; Gulik *et al.*, 1994), which lost their double-bilayer periodicity when all the chains became melted. The structure shown in Fig. 10 is consistent with the bilayer association as a result of the present proteins. The PLS-sample contains the proteins SP-B and SP-C, both of which are considered to link two apposing bilayers (Weaver, 1998), which can be expected to result in a rather short gap between the associated bilayers.

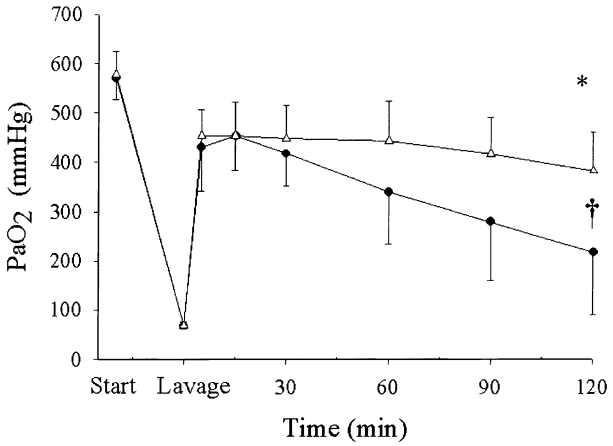

Figure 9 Change in mean PaO_2 values (±SD) over time of the two groups before lung lavage (start), after lavage (lavage) and after surfactant administration. Black circles group which received surfactant when steady-state was reached, open triangles group which received surfactant at maximum swelling of the PLS in saline solution. *$P<0{\cdot}01$ at 120 min between steady-state group and maximum swelling group, †$P<0{\cdot}001$ between 5 and 120 min in the steady-state group.

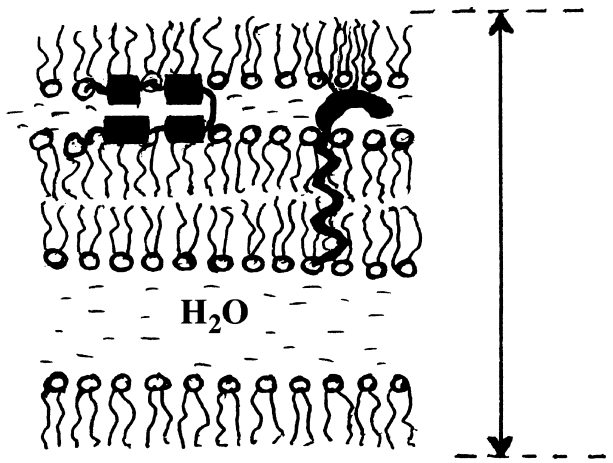

Figure 10 Structure of the PLS-water double-bilayer liquid-crystalline phase. The arrow to the right shows the lamellar unit period. The lipids are indicated by their polar head groups (circles) and the two liquid-like disordered hydrocarbon chains in each molecule. Protein molecules link two bilayers and the other bilayer gap contains water only. SP-B, considered to be located at the polar region, is shown to the left and SP-C is indicated to the right, with a helical segment spanning one bilayer and two palmitoyl chains embedded in the opposite monolayer (illustrated here as denser chain packing).

The cryo-TEM textures shown in Figs 7 and 8 confirm the proposed double-bilayer structure. A periodicity of about 120° is seen in Fig. 7 and also in the liposome-type of dispersion shown in Fig. 8. The two bilayers forming the vesicles shown in Fig. 7 form a remarkable linear structure when two vesicles fuse, forming a unit consisting of three bilayers (indicated by a circle in Fig. 7). The liquid-crystalline phase from which the vesicles are formed has a structure unit consisting of two non-equivalent bilayers, designed A and B, respectively, which means that the repetition of the double bilayers AB in this phase can be described as ..AB/AB/AB/.... If we move through the bilayers AB forming the surface of one vesicle and enter an apposing vesicle, the bilayers there are related by mirror symmetry to the first vesicle, i.e. they can be described as BA. The bilayers at the fusion region, which we denote//, cannot, however, be AB//BA, as the periodic order requires A and B to always alternate. A rearrangement into A//B//A is therefore needed. This mechanism can explain the triple-bilayer unit structure and the mirror symmetry at fusion shown in Fig. 7.

Our microscopy observations indicate that both the presence of the inorganic ions of Ringer or saline solution and the presence of a solid–liquid interface is needed for the remarkable formation of surface network textures described above. We believe that this process reflects the formation of a dynamically active state of PLS. Extraction in an organic solvent and evaporation, as in our PLS preparation, means that polar protein regions are turned inside and hidden by hydrocarbon regions. Such molecular complexes must drastically change their conformations in order to form bilayers, when exposed to water. When ions from saline or Ringer solution are present, they obviously contribute to the dissociation of these complexes. Furthermore, any reorganization process within the bilayer should be expected to be favoured by the presence of an air–water interface, as a result of the driving force to form the ideal surface structure. Inversely, spreading at an interface should be favoured by the dynamics involved in these conformational changes within the bilayer. Such improved spreading at the alveolar surface may explain our *in vivo* observations.

The cationic SP-B and SP-C should be expected to interact with anionic phospholipid head groups, and the presence of ions in saline or Ringer solution may induce dissociation of ionic PG/SP-B or PG/SP-C complex. Such interactions might be involved in the formation of the ordinary bilayer structures in Ringer and saline solutions.

There are also numerous studies of the effect of ions on well-defined phospholipid monolayer and bilayer structures. If, for example, charged (anionic) lipid species are present, calcium ions, as a result of electrostatic bridging of adjacent polar head groups, will contract the polar region. This will induce a favouring of reversed types of bilayer structures on behalf of the ordinary lamellar liquid-crystalline conformation, (cf. Larsson & Quinn, 1994). The calcium ion effect might also be related to specific effect on the surfactant system, (cf. Benson *et al.*, 1984).

Purified calf lung surfactant behaviour in electrolyte solution has been studied with regard to surface film formation (Davies *et al.*, 1986). The surface activity in distilled water was improved by the addition of calcium and magnesium ions at a concentration of 5·6 mM, whereas 20 mM of sodium ions was required. The adsorption of pulmonary surfactant in relation to bulk concentration of calcium ions in a surface balance has also been studied (Kobayashi & Robertson 1983). The adsorption rate on a hypophase of 0·9% sodium chloride was similar to that on the same hypophase with 0·05% calcium chloride added. The significance of calcium ions in reconstitution of tubular myelin from synthetic lipids and SP-A and SP-B has been demonstrated by Suzuki *et al.* (1989).

It has been demonstrated that (Bernhard *et al.*, 2000) *in vitro* function of several commercial surfactants could be improved by the addition of calcium and resulted in surface tensions more comparable with native surfactants. (The physiological calcium concentration in the alveolar space is approximately 1·5 mmol l^{-1} (Nielson & Lewis, 1988) and in the used Ringer solution 2·0 mmol l^{-1} which simulates alveolar conditions.)

Utilizing the *in vitro* observations of a time-related swelling behaviour, we used two time points (maximum swelling and steady-state) to instill the PLS saline mixture into an extensively studied and reproducible model of lung injury (8). PLS was mixed with saline because in surfactant replacement therapy only saline is used, and the dynamics in swelling behaviour was also observed with saline PLS mixture. To optimize the detection of any effect of the swelling behaviour on the surfactant function *in vivo*, we used a low dose of PLS which by itself was not enough to completely restore the induced lung injury, as shown by the PaO_2 data (Fig. 9). However, in both groups PaO_2 increased significantly after surfactant administration (Fig. 9). Over time the PLS mixture which had reached steady-state (under polarization microscopy) before administration PaO_2 levels dropped significantly during the 2-h study period. The level of PEEP in both groups was similar as was the lung injury induced by BAL. Therefore, we conclude that surfactant function represented by arterial oxygenation of the maximum swelling PLS condition is superior to the steady-state PLS condition. A possible explanation for the better effect of surfactant replacement during the dynamic swelling phase is that the dynamic swelling provides a better distribution of the instilled surfactant. The tree-like projections seen in Figs 4 and 5 extend over millimetres, i.e. over several alveolar diameters.

The most important result of this study is the demonstration of a variation of the physiological effects at administration in relation to the aqueous mixing time; a time which proved to be directly related to the dynamics of swelling observed *in vitro*. This means that lung surfactant extract preparations should be analysed with regard to the swelling dynamics in order to determine the maximum in dynamics, which was found to occur at the half-time of achievement of a steady-state. This predetermined time, which may vary from one production batch of PLS to the other, could enhance the therapeutic effect at administration.

Acknowledgements

This work was financially supported by the International Foundation for Clinically Oriented Research (IFCOR) and the Swedish Medical Research Council 10841.

The authors thank Stefan Krabbendam, Erasmus University Rotterdam, for expert technical assistance and Laraine Visser-Isles, Erasmus University Rotterdam, for English language editing. Leo Pharmaceutical Products, Denmark, kindly provided the porcine lung extract.

References

Amrein M, von Nahmen A, Sieber M. A Scanning force- and fluorescence light microscopy of the structure and function of a model pulmonary surfactant. *Eur Biophys J* (1997); **26**: 349–57.

Benson BJ, Williams MC, Suechi K, Goerke J, Sargeant T. Role of calcium ions in the structure and function of pulmonary surfactant. *Biochim Biophys Acta* (1984); **793**: 18–27.

Bernhard W, Mottaghian J, Gebert A, Rau GA, van Der Hardt H, Poets CF. Commercial versus native surfactants. Surface activity, molecular components and the effect of calcium. *Am J Respir Crit Care Med* (2000); **162**: 1524–1533.

Bligh EG, Dyer WJ. A rapid method of total lipid extraction and purification. *J Biochem. Physiol* (1959); **37**: 911–917.

Boncuk-Dayanikli, P, Teusch, H. Essential and nonessential constituents of exogenous surfactants. In: *Surfactant Therapy for Lung Disease* (eds Robertson B., Teusch H. W.) (1995); pp. 217–238. Marcel Dekker Inc., New York.

Davies RJ, Gengheni M, Walters DV, Morley CJ. The behaviour of lung surfactant in electrolyte solutions. *Biochim Biophys Acta* (1986); **12**: 135–145.

Gommers D, Lachmann B. Surfactant therapy: does it have a role in adults? *Clin Intensive Care* (1993); **4**: 284–295.

Gommers D, Vilstrup C, Bos JAH, *et al* Exogenous surfactant therapy increases static lung compliance, and cannot be assessed by measurement of dynamic compliance alone. *Crit Care Med* (1993); **21**: 567–574.

Gulik A, Tchoreloff P, Proust J. A conformation transition of lung surfactant lipids probably involved in respiration. *Biophys J* (1994); **67**: 1107–1112.

Janiak MJ, Small DM, Shipley GG. Nature of the thermal pretransition of synthetic phospholipids: dimyristoyl- and dipalmitoyllecithin. *Biochemistry* (1976); **15**: 4575–4579.

Kobayashi T, Robertson B Surface adsorption of pulmonary surfactant in relation to bulk-phase concentration and presence of Cacl2. *Respiration* (1983); **44**: 63–70.

Lachmann B, Robertson B, Vogel J. *In vivo* lung lavage as an experimental model of the respiratory distress syndrome. *Acta Anaesthesiol Scand* (1980); **24**: 231–236.

Larsson K, Quinn PJ. Physical properties: structural and physical characteristics. In: *Lipid Handbook* (eds Gunstone F. D., Harwood J. L., Padley F. B.) (1994); pp. 401–486. Chapman & Hall, London.

Mateu L, Luzzati V, London Y, Gould RM, Vosseberg FGA, Olive J. X-ray diffraction and electron microscopy study of the interaction of myelin

components. The structure of a lamellar phase with a 150–180° repeat distance containing basic proteins and acidic lipids. *J Mol Biol* (1973); **75**: 697–709.

von Nahmen A, Schenk M, Sieber M, Amrein M. The structure of a model pulmonary surfactant as revealed by scanning force microscopy. *Biophys J* (1997); **72**: 463–469.

Nielson DW, Lewis MB. Calcium increases in pulmonary alveolar fluid in lambs at birth. *Pediatr Res* (1988); **24**: 322–325.

Reiss OK, Paul GW, Gil J. An electron microscopic study of thin films of alveolar surfactants and dipalmitoyl phosphorylcholine. *Prog Respir Res* (1984); **18**: 29–35.

Suzuki Y, Fujita Y, Kogishi K. Reconstitution of tubular myelin from synthetic lipids and proteins associated with pig pulmonary surfactant. *Am Rev Respir Dis* (1989); **140**: 75–81.

Weaver TE. Synthesis, processing and secretion of surfactant proteins B and C. *Biochim Biophys Acta* (1998); **14908**: 173–179.